*J. Biomater. Sci. Polymer Edn*, Vol. 17, No. 1-2, pp. 121-137 (2006).

Also available online – www.vsppub.com

# Multiphase Blends from Poly(L-lactide) and Poly(methyl methacrylate)

KIM-PHUONG LE[1], RICHARD LEHMAN[1*], JESSICA REMMERT[2], KENNETH VANNESS[2], PAULA MARIE L. WARD[3], JAMES D. IDOL[1]

[1]*AMIPP Advanced Polymer Center, Rutgers University, 607 Taylor Road, Piscataway, NJ 08854.*
[2]*Department of Physics, Washington and Lee University, Lexington, VA*
[3]*Department of Biochemistry and Microbiology, Cook College/NJAES, Rutgers University, New Brunswick, NJ*

Received 7 December 2004; accepted 14 June 2005

**Abstract** — Melt processing of poly(L-lactide) (PLLA) and poly(methyl methacrylate) (PMMA) blends was conducted over a targeted range of compositions with PLLAs of 118 and 316 kg/mol molecular weight to identify morphologies and the phase relationships in these blends. These blends are of interest for use in biomaterials and the morphologies are critical for tissue engineering studies where biodegradability, pore connectivity, and surface texture control tissue viability and adhesion. Simple extrusion of the two polymers produced multi-phase blends with an average domain size near 25 microns. Scanning electron microscopy (SEM) and dynamic mechanical analysis (DMA) demonstrate that these blends are immiscible, at least in a metastable sense, and regions of co-continuous structures were identified. Such co-continuous regions, which occurred generally in accordance with rheology prediction models, exhibit a fine interconnected structure that appears attractive for fabricating certain biomaterials. A broad and unexpected transition appears in these blends, as measured by modulated differential scanning calorimetry (MDSC), between 70 $^{o}$C and 100 $^{o}$C that may be the glass transition ($T_g$) of an alloy phase. The magnitude of this transition is greatest in the fine structured co-continuous composition region of blends, suggesting the presence of a complex or other derivative of the two primary phases.

*Key words:* Polymer blend, extrusion, immiscibility, scaffold, tissue engineering, bioresorbable

## INTRODUCTION

Thermo-mechanical mixing of two or more polymers is a preferred new material development method since such blending does not involve costly synthesis and scale-up can be achieved quickly and inexpensively once promising blends have been

*To whom correspondence should be addressed. Tel.: (1-609) 203-2501; Fax: (1-732) 445-5584; E-mail: rllehman@rutgers.edu

identified. Such new materials, processed under the proper conditions, may exhibit synergistic and advantageous properties [1]. The resulting blends may or may not be miscible. Miscible blends and/or compatibilized immiscible blends are the main objectives for thermal blending, but uncompatbilized immiscible blends have recently gained significant attention [2] due to their ability to provide unexpected properties. Studies have shown that for certain applications, such as bone and tissue scaffolds, immiscible blends have specific advantages in morphological and mechanical properties. Presently, it is believed that the co-continuous nature of certain immiscible compositions gives rise to the synergistic properties, due to the intimate interaction between the components.

Numerous applications, in particular in the biomedical field, require porous materials to impart the desired biomedical functions, such as cell culturing and growth. The morphology of co-continuous immiscible blends is well suited to generate porous materials with interconnected channels by processing a two-phase composite with subsequent leaching of one phase. The pore size and porosity of the resulting porous matrices can be engineered based on the choice of the components, as well as processing and popst-processing techniques and conditions. A second class of *in vivo* applications requires load-bearing materials as substitutes or partial replacements for hard tissue. Such materials must have initial strength and stiffness comparable to the targeted hard tissue, but must also induce tissue growth to replace all or part of the implant over a suitable time interval. In this process, part of the original implant is resorbed by the body in a way that generates porosity and penetrating channels, such that tissue growth and adhesion is encouraged.

Multiphase polymer blends, in which one phase is transient and another phase is persistent, can provide the ideal balance of phases with the ratio modified to meet the specific application and to produce the desired results [3]. The initial processing of the blend is important and numerous physical properties of the polymers, in particular the rheology, are critical and determine the properties and morphology of the resultant blend. An additional issue that requires consideration is the nature of the phase interface in immiscible blends. A weak interface can have an adverse effect on the mechanical properties of the blend [4], whereas a non-bonded interface or even the development of reaction products at the interface can impart important functionality to the blend.

Still another group of biomedical applications, e.g., scaffoldings, requires exceptionally high levels of porosity (>70%) and are most effectively processed by combining a functional biomaterial polymer with an extractable second phase. Subsequent to the primary processing, the extractable phase is removed by leaching. Most preferably, this extractable phase is removed with a non-toxic solvent such as water, which requires that the extractable phase be water-soluble or water-degradable [5]. On the other hand, to take full advantage of thermal processing, this leached phase should also possess comparable mechanical properties and thermal processability. Only a few polymers fit into this category, mostly polyesters such as poly(lactide) (PLA, including poly(L-lactide) (PLLA) and poly(DL-

lactide (PLA)) and poly($\varepsilon$-caprolactone) (PCL) [6, 7]. PLA and its derivatives have quite attractive properties for these applications and have been the focus of considerable recent scientific study. A few examples of studied systems are PLLA/PCL [4], PLA/poly(methyl methacrylate) (PMMA) in solution and melt system [8], PLLA/poly(styrene) (PS) [9] and PLA/poly(ethylene glycol) (PEG) [10, 11].

Overall, the numerous studies of PLA materials, including neat PLA, PLA blends and PLA co-polymers, have produced a wide array of materials and a considerable body of papers in the literature. However, much about the physical behaviour of the PLA phase remains unclear. In particular, the effect of processing on the crystallinity and glass transition behavior are not well understood or documented. Furthermore, the coupling of these properties with molecular mass and monomer hydrophobicity is necessary to help understand the resultant mechanical properties, thermal properties, immiscibility with blend polymers and degradability [12–14].

Our research group is interested in immiscible polymer blends, their processing and properties. The premise guiding the current work is that the unique morphology achieved with the melt processing of immiscible polymers is approximately biomimetic and can be utilized to achieve novel and valuable properties in PLLA blends. In this work, we have selected PMMA as the second blend component, due to the fact that it is biocompatible, bio-inert and thermally processable with high-molecular-mass PLLA, thus providing an excellent polymer blend system for load-bearing implants that are partially resorbed at a rate compatible with tissue growth rates. Although immiscible polymer blends have traditionally been regarded as impractical due to poor adhesion between phases, e.g., work with PLLA/PCL blends [4], processing methods used in our laboratories have shown ways in which these limitations can be ameliorated.

## MATERIALS AND METHODS

### *Materials*

Extrusion-grade PMMA was obtained in the form of clear pellets (Atofina, Philadelphia, PA, USA). Two medical grades of PLLA, PLA L210 and PLA L207S, were obtained in the form of white granular powders (Boehringer-Ingelheim, Petersburg, VA, USA). Both grades are pure PLLA with molecular masses of 118 and 316 kDa, as shown in Table 1.

### *Rheology*

Rheology measurements were performed on all polymers over a range of shear rates and in the relevant temperature range (200–220°C). These data are necessary to determine the composition range over which co-continuous blends are expected. All rheology measurements were performed using a TA AR 2000 rheometer (TA, New Castle, DE, USA).

**Table 1.**
Viscosity and molecular mass of PLLA

| Chemical trade name | PLA L210 | PLA L207S |
|---|---|---|
| Boehringer material No. | 60640645 | 51923 |
| Lot No. | 1005490 | 1005010 |
| Inherent viscosity (dl/g) | 3.9 | 1.8 |
| Intrinsic viscosity (dl/g) | 4.2 | 1.9 |
| Mark–Houwink $K$ | $1.29 \times 10^{-4}$ | $1.29 \times 10^{-4}$ |
| Mark–Houwink $\alpha$ | 0.82 | 0.82 |
| Molecular mass (kDa) | 316 | 118 |

Inherent viscosity from Boehringer specification sheets. The value for L210 is the average value of viscosity range limits (3.4 and 4.4). The Mark–Houwink constants are from Ref. [15]. Instrinsic viscosity was estimated from inherent viscosity, which was measured at 0.1% concentration in chloroform at 25°C by the Solomon–Ciuta relationship [16].

**Table 2.**
Viscosity data measured with a TA AR-2000 rheometer to be used to predict co-continuous compositions

| | Raw material | | |
|---|---|---|---|
| | PLA L210 | PLA L207S | PMMA |
| Density (g/cm$^3$) | 1.25 | 1.25 | 1.18 |
| Viscosity (Pa·s) | 3739.2 | 1562.7 | 3989.1 |
| $\eta$(PLLA)/$\eta$(PMMA) | 0.937 | 0.392 | |
| Co-continuous composition (vol% PLLA) | 48.4 | 28.1 | |

Values obtained at 200°C and $\gamma = 78.5\ \mathrm{s}^{-1}$.

### *Blend formation*

Of all the immiscible blend compositions the compositions exhibiting co-continuous morphology generally have the best properties and various methods exist for approximating the composition of this region. One such method [17] identifies the region according to the following relationship between the volume fraction ($\Phi$) ratio and the viscosity ($\eta$) ratio of the components at the processing temperature:

$$\frac{\eta_A}{\eta_B} \cong \frac{\Phi_A}{\Phi_B}.$$

The PLLA/PMMA composition that conforms to this relationship is 48% for PLA L210 and 28% for PLA L207S, as shown in Table 2. The co-continuous composition is anticipated to provide not only the best mechanical properties, but also useful biomimetic structures resulting from the intertwining nature of the two phases in such blends. However, in addition to the co-continuous compositions estimated from the rheology data, other bracketing compositions were formulated, as shown in the complete list of blends in Table 3.

**Table 3.**
Composition of PLLA/PMMA blends

| Blend No. | PLA L210 | | PLA L207S | | PMMA | |
|---|---|---|---|---|---|---|
| | vol% | wt% | vol% | wt% | vol% | wt% |
| 1 | 100 | 100 | | | 0 | 0 |
| 2 | 58.38 | 59.8 | | | 41.62 | 40.2 |
| 3 | 53.38 | 54.8 | | | 46.62 | 45.2 |
| 4 | 48.38 | 49.8 | | | 51.62 | 50.2 |
| 5 | 43.38 | 44.8 | | | 56.62 | 55.3 |
| 6 | 38.38 | 39.8 | | | 61.62 | 60.2 |
| 7 | | | 100 | 100 | 0 | 0 |
| 8 | | | 38.15 | 39.5 | 61.85 | 60.5 |
| 9 | | | 33.15 | 34.4 | 66.85 | 65.6 |
| 10 | | | 28.15 | 29.3 | 71.85 | 70.7 |
| 11 | | | 23.15 | 24.2 | 76.85 | 75.8 |
| 12 | | | 18.15 | 19.0 | 81.85 | 81.0 |
| 13 | 0 | 0 | 0 | 0 | 100 | 100 |

*Extrusion*

The PLLA and PMMA polymers were dried overnight in a vacuum oven at 45 and 70°C, respectively, prior to processing. Batches of 110 g were weighed out and melt-processed in a 19-mm single-screw laboratory extruder (Brabender, Hackensack, NJ, USA) fitted with a mixing screw of 0.655 inch (1.67 cm) average root diameter. An average shear rate of 78.5 $s^{-1}$ was achieved at 200°C by operating the extruder at 100 rpm. No die was used and the processed polymer composite was extruded from the barrel opening as rods of approx. 13 mm in diameter. These rods were cut into convenient lengths and cooled under ambient conditions. These segments were then milled into smaller bars and discs for subsequent characterization. Other specimens were fractured in liquid nitrogen (77 K) and used for electron microscopy imaging.

*Characterization*

The structure and morphology of the blends were assessed with scanning electron microscopy (SEM) using a Hitachi 2700 microscope operated at 15 kV. Specimens were prepared from blends by cryo-fracture to obtain surfaces nearly representative of the bulk. All samples showed a strong skin–core morphology, a general feature of extruded composites of this type. The non-representative surface skin was removed by milling prior to cutting samples from the extrudate. The PLLA and PMMA phases were revealed for imaging purposes by etching with dimethyl formamide (DMF) for various times. A simple etch to reveal phases consisted of 1 min at 22°C, whereas longer times were used to completely remove the PMMA phase to the depth of SEM imaging. Images were taken parallel and perpendicular to the extrusion axis.

Crystallinity, glass transition and the presence of reaction product phases were examined by differential scanning calorimetry (DSC) using a TA Instruments Q1000. Sample discs (10 mg), approx. 5 mm in diameter and 0.4 mm thick, were prepared by cutting 0.4-mm cross-sectional wafers from the 13-mm cylindrical extruded rods and punching 5-mm discs with a hole puncher. Care was taken to avoid both the skin and the core portion of the extruded rods. After initial DSC runs to determine proper ramp rates and temperatures for the PLLA/PMMA system, all subsequent runs were conducted with modulated DSC (MDSC) to achieve maximum separation of reversing and non-reversing effects, such as glass transition and crystallization. All runs included an initial heat, followed by a cool and reheat. The data presented in this paper were collected from the MDSC reheat cycle. MDSC modulation parameters were: amplitude, 2°C; period, 40 s; ramp rate, 2°C/min and temperature range, 20–210°C.

Dynamical mechanical analysis (DMA) using a Perkin-Elmer 7E assisted in determining glass transition temperatures ($T_g$), particularly for phases such as PMMA, that have low enthalpic $T_g$ signature, and also to determine the elastic modulus. Two modes were used, flexure and parallel plate oscillation. The flexural tests were conducted in a 3-point bending geometry using specimens machined from the outer section of the extruded pieces measuring $1 \times 3 \times 20$ mm with the largest dimension parallel to the flow direction. Two types of flexural rests were run: (1) dynamic stress scans at room temperature at a strain rate of approx. 1.5 MPa/min up to strains of 0.25% and (2) temperature scans ramped at 5°C/min from room temperature up to approx. 90°C, while holding the strain constant at 0.025% (15 $\mu$m amplitude). For the parallel plate tests samples were machined from the extruded rods by making successive cuts perpendicular to the flow direction, resulting in discs approx. 1 mm thick and 10 mm in diameter. The latter were placed between 10-mm plates, subjected to sinusoidal strains (shear and compressive) of approx. 0.25% (2.5 $\mu$m amplitude) and heated at 5°C/min from room temperature to 200°C. The parallel plate tests were also conducted at 1 Hz.

## RESULTS AND DISCUSSION

### *Blend morphology by SEM*

Micrographs of the PLLA/PMMA composite at 28 vol% PLLA are shown in Fig. 1. The structure of the blends is clearly immiscible and co-continuous as evident from the web-like nature of the brighter phase and the penetrating continuous nature of the phase extracted by the etching agent, DMF. Pore size covers a wide range, from approx. 2 to 50 $\mu$m, with an average around 25 $\mu$m.

Varying levels of co-continuity were observed over range of compositions in both the PLA L207S/PMMA and the PLA 210/PMMA systems, although exact definition of the point of co-continuity was determined by DMA (see following section) rather than image analysis. These blends are naturally quite anisotropic

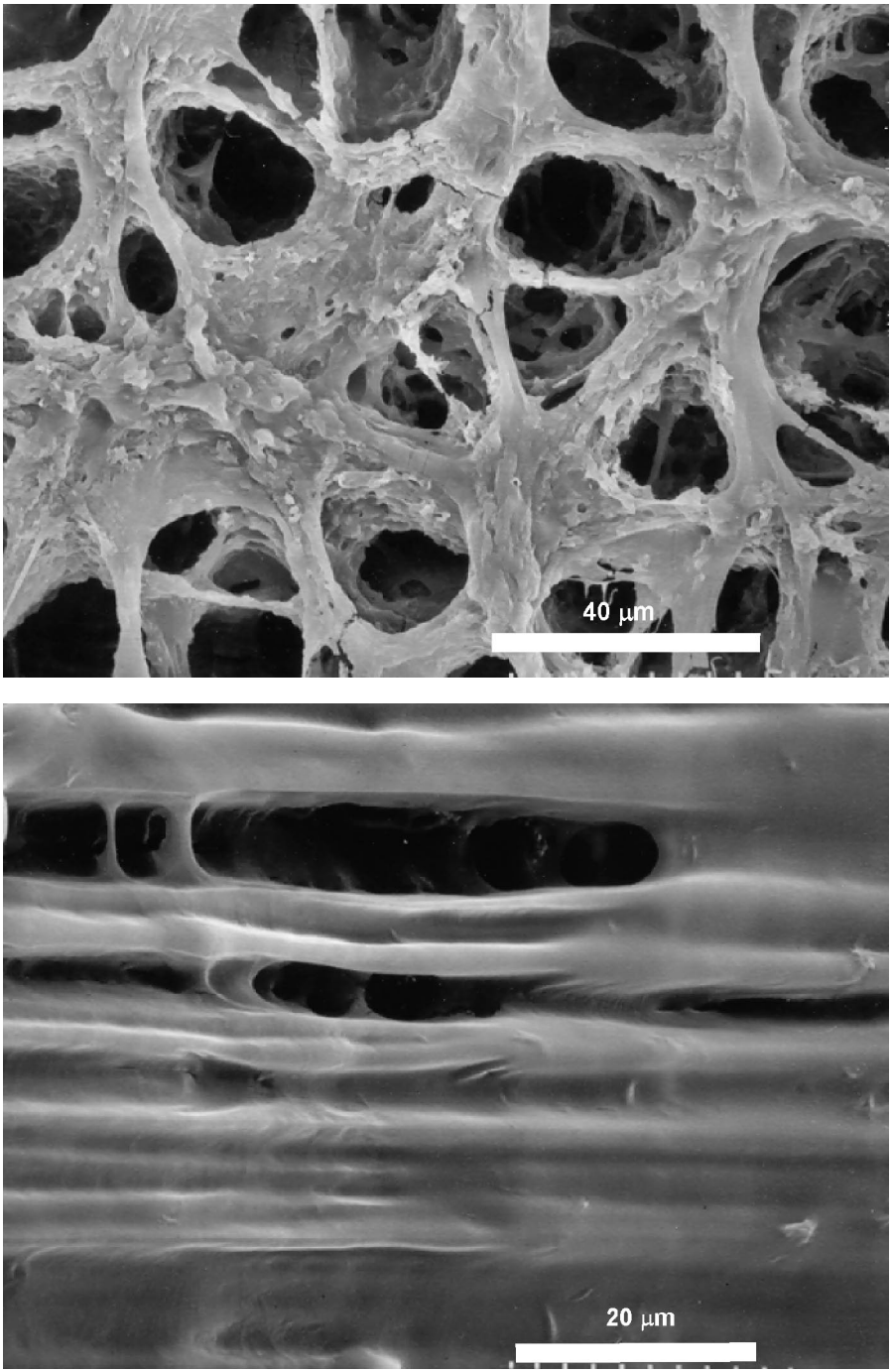


**Figure 1.** (Top) 28/72% (v/v) PLLA/PMMA composite: DMF etched, sectioned perpendicular to extrusion axis. (Bottom) 28/72% (v/v) PLLA/PMMA composite: DMF etched, sectioned parallel to extrusion axis.

with very different morphologies in the plane perpendicular to the extrusion axis (radial plane, Fig. 1, top panel) compared to the plane parallel to the axis ($z$-axis, Fig. 1, bottom panel). Clearly, the co-continuous structure of these blends consists of columnar strands, roughly oriented along the $z$-axis, intertwined with a web-like matrix. Although the micrographs of Fig. 1 strongly suggest co-continuity, no quantitative attempt has yet been made to verify this experimentally. This interesting structure is anticipated from the nature of the extrusion process and may provide particular functionality in biomaterial systems, a subject of on-going study in our laboratory.

*DMA, immiscibility and co-continuity*

When two polymers are combined in a blend, either a single-phase alloy forms or the polymers are immiscible in which case the $T_g$ of each component is readily apparent in the blend. Thus, monitoring of $T_g$ is an effective way to assess the immiscibility or alloying of polymer blends. Although the photomicrographs show compelling evidence of immiscibility, only the observance of two $T_g$ values is proof of a two amorphous phase structure. DMA results from flexural experiments (Fig. 2, top panel) at low temperature and from parallel plate experiments (Fig. 2, bottom panel) at high temperature illustrate the presence of multiple glassy phases in the 28 vol% PLA L207S blend. As is evident from subsequent data presented in this paper, e.g., DSC data, this 28% blend contains a substantial amount of reaction product or compatibilized mix of PLLA and PMMA that provides several $T_g$ values over the thermal spectrum. This effect may be seen in the flexural DMA data as the loss modulus spans a considerable temperature range, beginning at 62°C (PLLA $T_g$) and peaking near 80°C. The storage modulus and tan $\delta$ behavior accordingly. Flexural DMA was not useful above 95°C, since a large amount of liquid developed in the composite by the time this temperature was reached and, hence, it was no longer suitable for beam-bending measurements. For these higher temperature measurements we switched to the parallel plate DMA method, which was quite useful to assess the PMMA $T_g$, since the blend is nearly all liquid at this point with only the PLLA crystalline phase remaining. The peak in the parallel plate storage modulus data is an artifact of the measurement, since some liquid phase is required to provide proper mechanical linkage between the sample and the parallel plates. Once this point is reached, the amount of liquid phase is already increasing and the storage modulus curve decreases accordingly. The asymmetry of the loss modulus curve reveals the presence of the intermediate $T_g$ values on the low temperature side and the prominence of the PMMA $T_g$ at 104°C. Tan $\delta$ decreases at temperatures above 116°C, apparently due to recrystallization of PLLA.

In addition to determining $T_g$ values, DMA is an effective tool to assess the composition at which an immiscible polymer blend is co-continuous. In scanning the entire range of a two-component composition, co-continuity is expected near the point of phase inversion where one phase transitions from the dispersed phase to the continuous phase. In this special composition range both phases are continuous

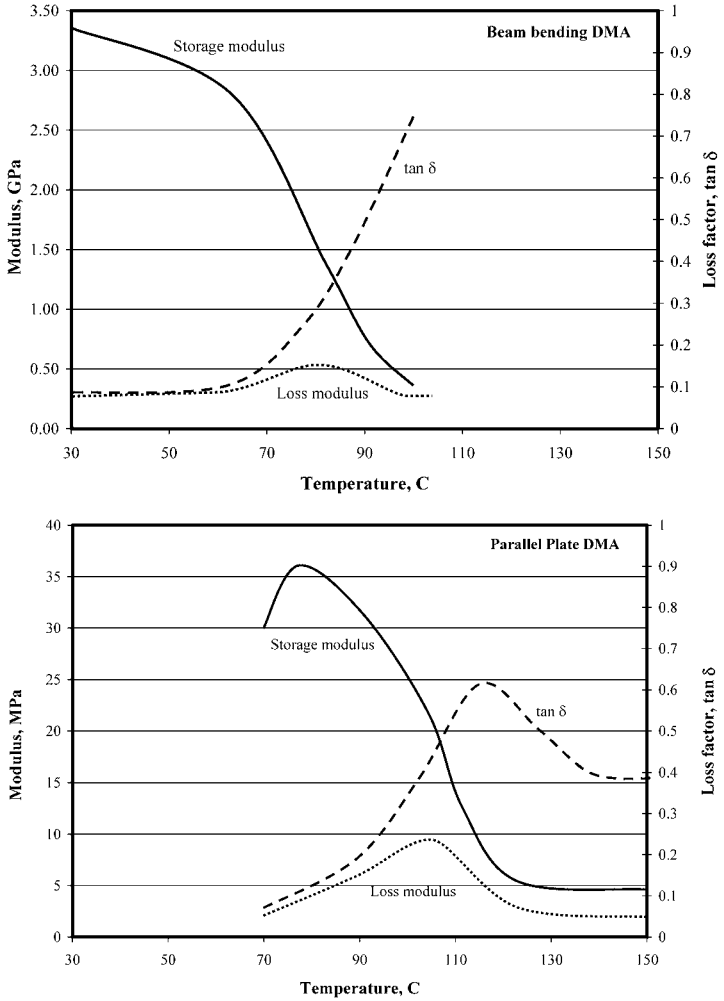


**Figure 2.** (Top) Flexural DMA data on PLA L207S/PMMA composite (28 vol% PLLA), illustrating low-temperature transitions. (Bottom) Parallel-plate DMA data on PLA L207S/PMMA composite (28 vol% PLLA), illustrating high-temperature transitions.

and intertwined, thus providing a unique architecture wherein mechanical load is efficiently transferred between phases. DMA capably identified the co-continuity region for the blends of PMMA with PLA L207S and PLA L210 (Fig. 3), as evidenced by the rapid increase in storage modulus as co-continuity is achieved. The DMA modulus maxima for composites prepared from PLA L207S and PLA L210 occur approximately at 33 and 43 vol%, respectively, in close accord with the predictions of the Jordhamo relationship. Thus, these data confirm the region of co-continuity directly and also indirectly provide additional evidence of the immiscible structure of these blends.

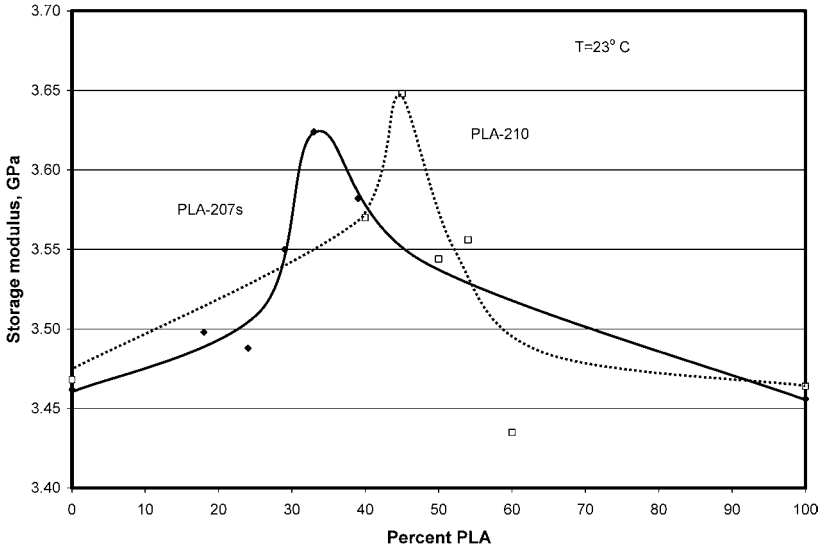


**Figure 3.** Storage modulus by DMA for PLLA/PMMA blends. Regions of phase co-continuity are shown by maxima.

*DSC and amorphous phase relationships*

The thermal analyses of the PLLA/PMMA blends revealed several interesting features. The $T_g$ of the semicrystalline PLLA is a strong enthalpic signature and is readily observed as the derivative of the reversing MDSC heat flow (Fig. 4) at 62°C. The full width at half maximum (FWHM) for this $T_g$ is 6°C, an indicator of the degree to which comparable $T_g$ values can be differentiated. As noted previously, the $T_g$ of PMMA is not as strong and although it clearly appears when neat PMMA is analyzed, it is not well defined in the PLLA/PMMA blends. What does appear for the PLA L207S blends is a broad derivative heating endotherm centered near 85°C and extending from 70 to 100°C. This endotherm has not been previously reported and represents a new finding in the current work. Since the maxima are endothermic, reversing and observed on reheat, we hypothesize that these endotherms may represent the glass transition for either a new phase that has formed in the blend during processing or a region of partial miscibility and compatibilization between PLLA and PMMA. In this discussion we refer to this additional new phase as PG80.

In Fig. 4 (top panel) the DSC curves for the PLA L207S blends are presented and labeled at 62 and 105°C, the PLLA and PMMA $T_g$ points, respectively, according to the sequence of the curves at those temperatures. At 105°C the curves are in order of PMMA concentration, suggesting an overlap of the 85°C maximum with the subtle PMMA $T_g$ and/or a key role of PMMA as a reactant in forming PG80 during processing. At 62°C the order of the curves does not correlate directly with blend PLLA concentration but rather varies with PLLA concentration and inversely

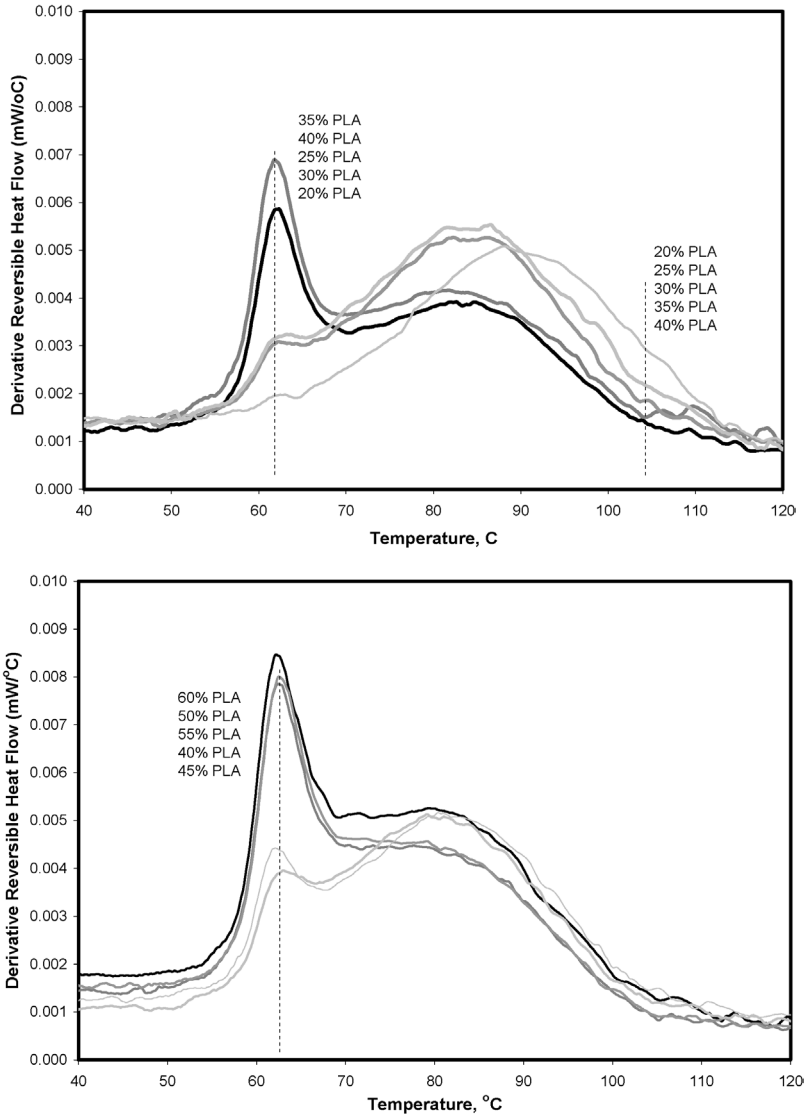


**Figure 4.** (Top) Derivative of reversing heat flow from MDSC analysis of PLA L207S/PMMA blends. (Bottom) Derivative of reversing heat flow from MDSC analysis of PLA L210/PMMA blends.

with the intensity of the PG80 $T_g$. The greatest PG80 DSC signal and, hence, the greatest PG80 concentration occurs at 25–30% PLLA, at or near the region of co-continuity in these blends. This behavior may be expected, since the intimate contact of co-continuous phases provides a high level of interfacial surface area at which the reaction between PLLA and PMMA can occur.

The PLA L210/PMMA blends behave similarly to the PLA L207S blends but with significant differences. PLA L210 is higher in molecular mass than PLA L207S

and as such it will be less reactive and have higher viscosity. The DSC curves (Fig. 4, bottom panel) show a strong, sharp PLLA peak at 62°C, consistent with the high concentration of PLLA in these blends. The PG80 maxima are, however, not as intense as for PLA L207S blends. This diminished production of PG80 may result either from the lower activity of PLA L210 or from the lower concentration of PMMA, suggesting a critical dependence of PG80 formation on PMMA either by virtue of reaction kinetics or precursor structure.

The degree to which PG80 is produced in the PLA L210/PMMA blends again depends strongly on the co-continuity of the structure and the intimacy of the phases under this condition. The 40–45% PLLA blends converted a greater proportion of PLLA to PG80 than any of the other compositions, as measured by a reduced PLLA $T_g$ at 62°C and a large PG80 $T_g$ at 80°C.

Quantification of the DSC data was accomplished by deconvoluting the derivative reversing heat flow curves using a normal distribution model for the constituent derivative heat flows. By employing best fit techniques good deconvolution results were obtained with PLLA curves centered at 62°C with $\sigma = 2.2$, PG80 centered at 77°C with $\sigma = 11.5$ and PMMA varied in the range of 90–100°C with $\sigma = 6$. An example of the method is shown in Fig. 5. The area under the curves represents the heat flux for the respective transition under the experimental DSC conditions employed. The integrated intensities are graphed in Fig. 6 for the PLA L207S blends (Fig. 6, top panel) and the PLA L210 blends (Fig. 6, bottom panel). Both graphs show similar trends. PG80 is a highly enthalpic phase and dominates the heat flow, comprising over 90% of the heat flow signature at the composition corresponding to co-continuity, about 25 and 45 vol% PLLA for PLA L207S and PLA L210, respectively. This is in excellent agreement with DMA co-continuity data (Fig. 3)

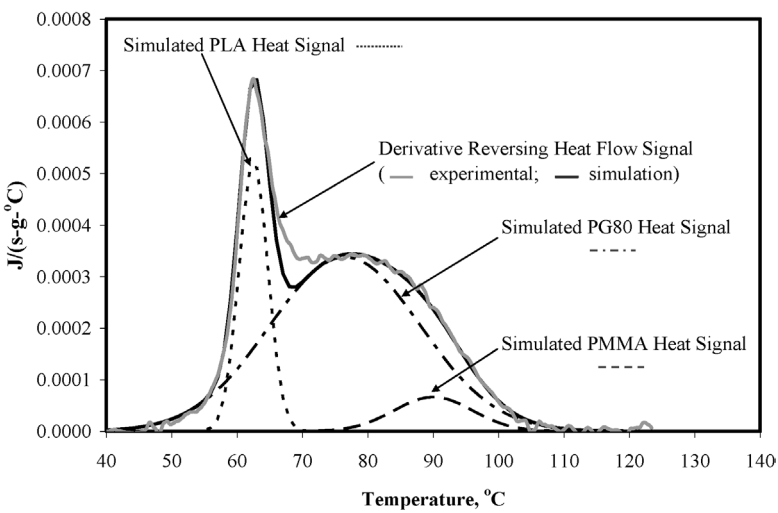


**Figure 5.** Example of DSC curve deconvolution using normal distribution function simulations of constituent $T_g$ derivative heat signals.

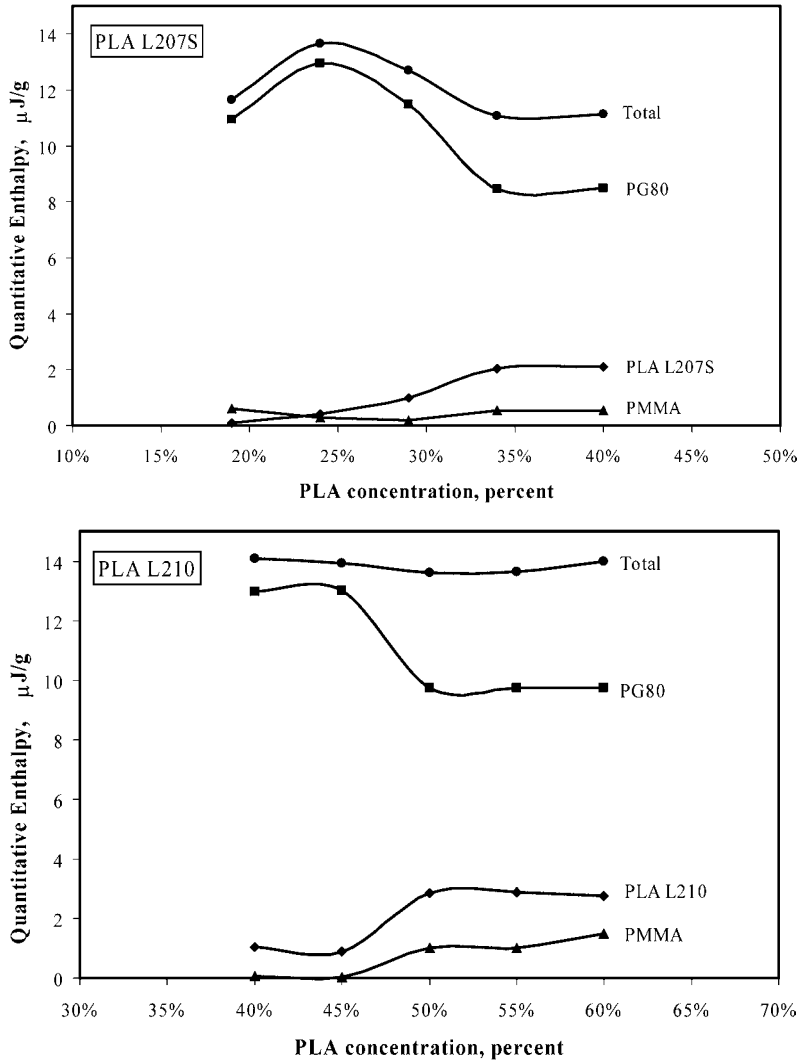


**Figure 6.** (Top) Quantitative DSG data for PLA L207S/PMMA blends illustrating PG80 maximum near the co-continuous composition. (Bottom) Quantitative DSG data for PLA L210/PMMA blends illustrating PG80 maximum near the co-continuous composition.

for the PLA L210 series and about 5% lower than the DMA data for the PLA L207S series. As the level of PLLA is increased beyond the co-continuous point the PG80 enthalpy drops and the signal from the PLLA and the PMMA increases, as expected from simple reactant/product relationships. Presumably symmetric relationships exist well below the region of co-continuity, although the current study did not include sufficient compositions in this region to permit a definitive statement to be made.

*DSC and crystallinity*

Crystallinity of the polymer blends is of interest, since this information can reveal important details regarding the processing and structure of the blends. The PLLA received from the supplier possessed high crystallinity, approximately 50% for both types, which reveals the slow cooling and/or annealing below $T_m$ the material was subject to during manufacture. When these polymers were extruded into PLLA/PMMA blends, the crystallinity level was much lower, 23 and 17% for PLA L207S and PLA L210, respectively, in accordance with the rapid post extrusion cooling and the differing molecular weights of the PLLA polymers.

The structure of the blend can also have marked effects on component crystallinity. When fine-structured immiscible co-continuous blends are processed, the spatial constraints imposed by sub-micron domains and the mechanical forces imposed by expansion and contraction can affect the crystallinity [18]. Conversely, the structure of a blend can be inferred to some degree from the crystallinity. The PLLA/PMMA blends studied show a suppression of crystallinity (Fig. 7) in the regions of co-continuity, about 35 and 45% PLLA for the 207S and 210 blends, respectively. Thus, the PLLA in co-continuous blends of PLLA/PMMA is essentially amorphous with the overall blends containing only 1–2% crystalline PLLA. This feature will have important implications regarding the behavior of these composites when chemically leached or when inserted *in vivo*.

*Cell growth and adhesion: preliminary study*

*Method.* In addition to the morphology and physical properties of these blends, their compatibility with relevant biological cells is an important aspect of this

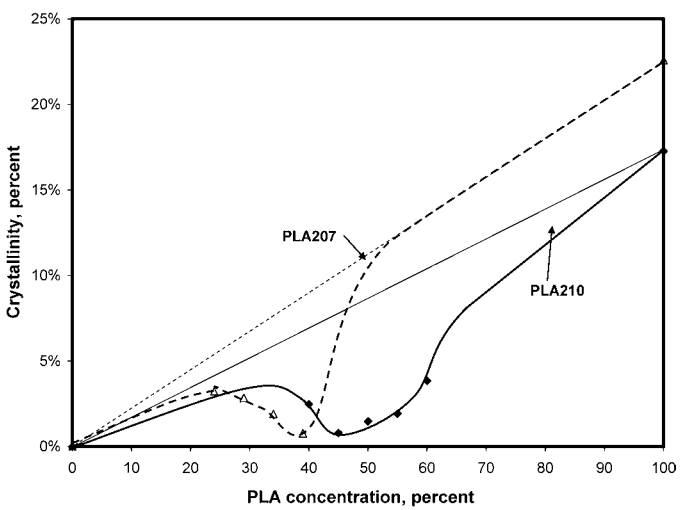


**Figure 7.** PLLA crystallinity *versus* percentage of the blend. Straight lines show expected behavior based on crystallinity of pure blend compositions.

research. Although the main thrust of the current study was to research and characterize the physical aspects of the polymer system, a preliminary study was conducted to determine if muscle and bone cells could survive and grow in the polymer environment. Furthermore, we sought to develop a procedure to measure cell adherence to the polymer blends, a critical characteristic for successful in vivo use.

Available muscle (C2C12) and bone (MC3T3-E1) cells were selected for the experiments, to mimic the soft and hard tissue exposures that would be anticipated under bone replacement conditions. Untreated cell, positive (12-O-tetradecanoyl phorbol 13-acetate, tumor growth accelerant) and negative (cycloximide, growth inhibitor) controls were included as experiment treatments to provide baselines, along with assay reagent controls.

The experiments were run one time to give an indication of whether further in-depth experimentation should be continued. Although experiments were run once, cell and control treatments were run in triplicate. Five treatments were included in the cell culture data, three neat polymers and two blends as indicated in Table 4. Specimen disks measured 7 mm in diameter by 1 mm thickness.

Cell viability was measured by adenosine 5′-triphosphate (ATP) quantification against controls. Supernatant from primary cell detachment was assayed once from each of the two cell types to ascertain positive growth, by reading through a luminometer.

Cell adhesion was measured by a special procedure developed to accommodate the opaque nature of the polymer blend specimens which precluded the conventional microscopy technique. Adhesion was determined by counting cells that remained in disk inclusions after all cells were initially trypsinized from the specimens and plate wells. To achieve this, the disks were isolated in 1.5-ml centrifuge capsules and further trypsinized prior to centrifuge separation. The cells were resuspended for hemocytometric quantitation.

*Results.* Hemocytometer cell counts and average luminescence readings ($n = 3$, mean standard error $= 27$) for each polymer blend treatment are shown in Table 4 by cell type. Although mean differences between the data were not replicated sufficiently to ascribe statistical differences or significance, trends were observed among cell types between polymer blends. Cells grew under all polymer treatments, indicating good compatibility of these materials to the two cell types studied. The smooth glassy surface of pure PMMA appears to restrict the attachment or adherence of both muscle and bone cells, when compared to pure PLLA polymers and blends. In general bone cells tended to adhere in greater numbers than muscle cells (Table 4, adhesion). It is also of interest to note a distinction between PLA L207 and PLA L210 exposure to cells. The attachment of both muscle and bone cells appears higher when exposed to PLA L210 over PLA L207. Although preliminary data suggest that the polymer blends support the *in vitro* growth of the two cell lines studied and that enhanced adhesion is observed in some blend

**Table 4.**
Preliminary adhesion and growth data for muscle and bone cells in contact with PLLA/PMMA polymer blends

| Treatment (polymer) | PLLA (%) | Cell line | Adhesion by hemocytometer | ATP by luminescence |
|---|---|---|---|---|
| PMMA | 0 | C1C12 | 14 | 455 |
| PLA L210 | 100 | C1C12 | 88 | 450 |
| PLA L207S/PMMA | 29 | C1C12 | 100 | 563 |
| PLA L207S | 100 | C1C12 | 141 | 409 |
| PMMA | 50 | C1C12 | 166 | 703 |
| PMMA | 0 | MC3T3-E1 | 14 | 543 |
| PLA L210 | 100 | MC3T3-E1 | 55 | 558 |
| PLA L207S/PMMA | 29 | MC3T3-E1 | 303 | 444 |
| PLA L210/PMMA | 50 | MC3T3-E1 | 339 | 327 |
| PLA L207S | 100 | MC3T3-E1 | 351 | 412 |

compositions, further study is necessary to quantitatively define the performance of these blends with regard to cell viability, adhesion and proliferation.

## CONCLUSIONS

Multi-phase blends of PLLA and PMMA which exhibit novel morphologies that appear to have value in biomaterial applications were prepared conveniently and economically using simple extrusion equipment. Scanning electron microscopy, as well as DMA demonstrates that these blends are immiscible, at least in a metastable sense, and regions of co-continuous structures were identified. Such co-continuous regions, which occurred generally in accordance with rheology prediction models, exhibit a fine interconnected structure that appears attractive for fabricating certain biomaterials. A broad and unexpected transition appears in these blends between 70 and 100°C that may be associated with the formation of an alloy phase. This phase, termed PG80, may be forming at the PLLA/PMMA interface as a complex or other derivative product of the two primary phases, particularly since the amount of PG80 is greatest in the intimately intertwined co-continuous range and since a qualitative inverse reactant/product relation exists between the areas under the PLLA and PG80 transitions.

*Acknowledgements*

The authors wish to thank Jessica Remmert for her work in performing DMA and SEM analysis, Prof. Thomas Nosker for advice on the experimental work, particularly the preparation of the blends, Prof. Michelle Marcolongo for her knowledge and direction regarding biological systems and Dr. Jennifer Lynch for guidance and assistance in the DSC laboratory. All DMA, SEM and extrusion work

discussed in this article was conducted at Washington and Lee University. We deeply appreciate the funding from the New Jersey Commission on Science and Technology, as well as major supporting equipment grants from TA Instruments, that made this work possible.

## REFERENCES

1. P. Martin, P. J. Carreau and B. D. Favis, *J. Rheol*. **44**, 569 (2000).
2. C. W. Macosko, *Macromol. Symp*. **149**, 171 (2000).
3. R. L. Lehman, J. D. Idol, T. J. Nosker and R. F. Renfree, US Patent Apllication 60/385,883 (2002).
4. R. Dell'Erba, G. Groeninckx, G. Maglio, M. Malinconico and A. Migliozzi, *Polymer* **42**, 7831 (2001).
5. N. R. Washburn, C. G. Simon Jr., A. Tona, H. M. Elgendy, A. Karim and E. J. Amis, *J. Biomed. Mater. Res*. **60**, 20 (2002).
6. D. W. Hutmacher, *Biomaterials* **21**, 2529 (2000).
7. K. J. L. Burg, S. Porter and J. F. Kellam, *Biomaterials* **21**, 2347 (2000).
8. G. Zhang, J. Zhang, S. Wang and D. Shen, *J. Polym. Sci. Part B Polym. Phys*. **41**, 23 (2003).
9. P. Sarazin and B. D. Favis, *Biomacromolecules* **4**, 1669 (2003).
10. Y. Hu, Y. S. Hu, V. Topolkaraev, A. Hiltner and A. Baer, *Polymer* **44**, 5711 (2003).
11. M. Sheth, R. A. Kumar, V. Dave and S. P. McCarthy, *J. Appl. Polym. Sci.* **66**, 1495 (1997).
12. H. Tsuji, K. Ikarashi and N. Fukuda, *Polym. Degrad. Stabil*. **84**, 515 (2004).
13. H. Urayama, T. Kanamori and Y. Kimura, *Macromol. Mater. Eng*. **286**, 705 (2001).
14. L. G. Griffith, *Acta Mater.* **48**, 263 (2000).
15. W. Dittrich and R. C. Schulz, *Angew. Makromol. Chem*. **15**, 109 (1971).
16. O. F. Solomon and J. Z. Ciuta, *Appl. Polym. Sci*. **6**, 683 (1962).
17. G. M. M. Jordhamo and L. H. Sperling, *Polym. Eng. Sci*. **26**, 517 (1986).
18. J. Joshi, R. L. Lehman and T. J. Nosker, *J. Appl. Polym. Sci.* (2006) (in press).